

Highly Entangled Photons and Rapidly Responding Polarization Qubit Phase Gates in a Room-Temperature Active Raman Gain Medium

Chao Hang^{1,2} and Guoxiang Huang^{1,3*}

¹*State Key Laboratory of Precision Spectroscopy and Department of Physics,
East China Normal University, Shanghai 200062, China*

²*Centro de Física Teórica e Computacional, Universidade de Lisbon,*

Complex Interdisciplinary, Avenida Professor Gama Pinto 2, Lisbon 1649-003, Portugal

³*Institute of Nonlinear Physics, Zhejiang Normal University, Jinhua, 321004 Zhejiang, China*

(Dated: November 9, 2018)

We present a scheme for obtaining entangled photons and quantum phase gates in a room-temperature four-state tripod-type atomic system with two-mode active Raman gain (ARG). We analyze the linear and nonlinear optical response of this ARG system and show that the scheme is fundamentally different from those based on electromagnetically induced transparency and hence can avoid significant probe-field absorption as well as temperature-related Doppler effect. We demonstrate that highly entangled photon pairs can be produced and rapidly responding polarization qubit phase gates can be constructed based on the unique features of enhanced cross-phase modulation and superluminal probe-field propagation of the system.

PACS numbers: 42.50.Ex, 03.67.Lx, 42.50.Gy

I. INTRODUCTION

Efficient schemes for producing entangled photons and constructing all-optical quantum gates are very important in optical quantum information processing and computation [1]. For this aim, a significant suppression of optical absorption and a giant enhancement of Kerr nonlinearity is crucial. However, in a conventional medium this can not be efficiently implemented because optical fields far away from atomic resonance are used to avoid large optical absorption, and hence the Kerr nonlinearity of the system is usually very weak.

In recent years, much attention has been paid to the study of electromagnetically induced transparency (EIT) in resonant atomic systems [2, 3]. The wave propagation in EIT media possesses many striking features, such as the large suppression of optical absorption, the significant reduction of group velocity, and the giant enhancement of Kerr nonlinearity [2]. Based on these features, many EIT-based applications, including optical quantum memory [4], high-efficient multi-wave mixing [2], optical atomic clocks [5–7], and slow-light solitons, etc. [8–11], have been intensively studied. Moreover, EIT-based schemes for producing entangled photons [12–14] and polarization qubit quantum phase gates (QPGs) [15–18] have also been proposed. However, the EIT-based schemes have some inherent drawbacks, such as the probe attenuation and spreading at room temperature and the long response time due to the character of ultraslow propagation [19]. These drawbacks impede the potential applications of EIT media for rapidly responding all-optical devices at room-temperature.

In this work, we shall propose a scheme to realize

highly efficient entangled photons and rapidly responding polarization QPGs in a resonant atomic system. The new scheme is based on active Raman gain (ARG) (or gain-assisted) configurations, which was demonstrated to be able to produce stable superluminal propagations of optical waves [20–25]. Contrary to the EIT-based schemes where the probe field operates in an absorption mode, the key idea of the ARG-based schemes is that the probe field operates in a stimulated Raman emission mode. Thus, they can avoid to be affected by a temperature related Doppler effect and significant probe field attenuation or distortion. Recently, it has been shown by Deng *et al.* [26, 27] that large and rapidly responding cross-Kerr effect are possible in ARG-based media. In addition, superluminal optical solitons are also predicted in such systems [28, 29]. Our system suggested here is a four-state tripod-type atomic one with a two-mode pump field and two weak fields. We shall prove that the unique features of the present system can be used to produce highly entangled photon pairs and implement rapidly responding polarization QPGs. Contrary to the entangled photons and QPGs in EIT media [15–18], the present ARG scheme has the following advantages: (i) It is able to eliminate the significant probe attenuation and distortion induced by temperature related Doppler effect, hence we can produce entangled photons with high degree and implement QPGs with high reliability at room temperature; (ii) It allows superluminal wave propagation, hence one can implement QPGs with very rapid response. The results presented in this work may be useful for guiding related experiments and facilitating practical applications in quantum information science [30].

The paper is organized as follows. In the next section we give a description of the model under study, and present the expressions of electric susceptibilities and the group velocity of probe and signal fields. In Sec. III, we describe a method to produce entangled superlumi-

*Electronic address: gxhuang@phy.ecnu.edu.cn

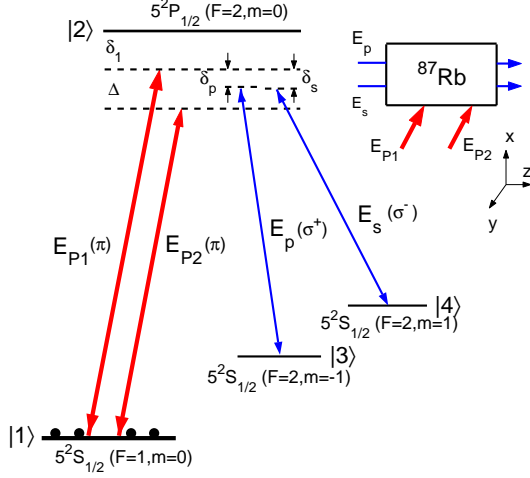


FIG. 1: (Color online) The energy levels $|l\rangle$ ($l=1-4$) and excitation scheme of the life-time broadened four-state tripod-type atomic system interacting with a strong continuous-wave two-mode pump laser field (with electric fields E_{P1} and E_{P2}) and two weak, pulsed (probe and signal) fields (with electric fields E_p and E_s). E_{P1} and E_{P2} are of π -polarization, while E_p (E_s) is of σ^+ (σ^-) polarization. δ_1 , δ_p , δ_s , and Δ are detunings. The inset shows a possible geometry of experimental set.

nal photons and construct polarization QPGs based on the present ARG system. In the last section, we provide a simple discussion on the temperature related Doppler effect and quantum noises. The main results of our research are also summarized.

II. THE MODEL AND LINEAR AND NONLINEAR SUSCEPTIBILITIES

We start with considering a life-time broadened four-level tripod-type atomic gas interacting with a strong continuous-wave two-mode pump laser field (with electric fields E_{P1} and E_{P2}), and two weak, pulsed laser (probe and signal) fields (with electric fields E_p and E_s), as shown in Fig. 1. The pump fields E_{P1} and E_{P2} are of π -polarization and couple the ground state $|1\rangle$ to the excited state $|2\rangle$ with large one-photon detunings δ_1 and $\delta_1 + \Delta$ ($|\Delta| \ll |\delta_1|$), respectively. The probe (signal) field E_p (E_s) is of σ^+ (σ^-)-polarization and couples the excited state $|2\rangle$ to the hyperfine state $|3\rangle$ ($|4\rangle$) with a two-photon detuning δ_p (δ_s). The system contains two Raman resonances due to the two-mode pump field for each weak field. Our scheme can be realized by a specific implementation using the D1 line of ^{87}Rb , where a homogeneous magnetic field parallel to the laser propagation direction is applied to encode binary information and avoid the undesirable couplings. A possible geometry of experimental arrangement is suggested in the inset of the figure. Note that the system we are considering here is a direct extension (by adding a new, weak signal field) of that used by Wang *et al.* [22] for the remarkable observation of stable, superluminal light propagation in

an ARG system.

The evolution equations for the atomic probability amplitudes $a_l(t)$ ($l=1-4$) are

$$\dot{a}_1 = \frac{\gamma_1}{2} a_1 + i\Omega_{P1}^* e^{i\delta_1 t} a_2 + i\Omega_{P2}^* e^{i(\delta_1 + \Delta)t} a_2, \quad (1a)$$

$$\dot{a}_2 = -\frac{\gamma_2}{2} a_2 + i\Omega_{P1} e^{-i\delta_1 t} a_1 + i\Omega_{P2} e^{-i(\delta_1 + \Delta)t} a_1 + i\Omega_p e^{-i(\delta_1 + \delta_p)t} a_3 + i\Omega_s e^{-i(\delta_1 + \delta_s)t} a_4, \quad (1b)$$

$$\dot{a}_3 = -\frac{\gamma_3}{2} a_3 + i\Omega_p^* e^{i(\delta_1 + \delta_p)t} a_2, \quad (1c)$$

$$\dot{a}_4 = -\frac{\gamma_4}{2} a_4 + i\Omega_s^* e^{i(\delta_1 + \delta_s)t} a_2, \quad (1d)$$

where $\Omega_{Pn} = -D_{21}\mathcal{E}_{Pn}/(2\hbar)$ ($n = 1, 2$), $\Omega_p = -D_{23}\mathcal{E}_p/(2\hbar)$, and $\Omega_s = -D_{24}\mathcal{E}_s/(2\hbar)$ are half-Rabi frequencies for $|1\rangle \leftrightarrow |2\rangle$, $|3\rangle \leftrightarrow |2\rangle$, and $|4\rangle \leftrightarrow |2\rangle$ transitions, with relevant electric dipole moments D_{21} , D_{23} , and D_{24} , and electric-field envelopes \mathcal{E}_{Pn} , \mathcal{E}_p , and \mathcal{E}_s , respectively. The detunings are defined by $\delta_1 = \omega_{21} - \omega_{P1}$, $\Delta = \omega_{21} - \omega_{P2} - \delta_1$, $\delta_p = \omega_{23} - \omega_p - \delta_1$, and $\delta_s = \omega_{23} - \omega_s - \delta_1$ (see Fig. 1). γ_1 presents the gain of state $|1\rangle$ for describing the effect of atoms going back to the ground state before being excited again. γ_l ($l = 2 - 4$) present the decay rates of state $|l\rangle$ for describing the effects of both spontaneous emission and dephasing. In the present work, we are interested in a closed system, i.e., there is no decay to levels outside the system we study, and hence γ_1 can be determined by the decay rates of higher states γ_l ($l = 2 - 4$) through the conservation of particle number $\sum_{l=1}^4 |a_l|^2 = 1$ [see Eq. (3) below]. Notice that here we employ the amplitude variable approach for the description of the motion of atoms and γ_l are introduced in a phenomenological manner. A complete description to include spontaneous emission and dephasing can be obtained by a density-matrix equation approach. However, for the ARG-based coherent atomic systems, two approaches are equivalent.

In order to investigate the propagation of the probe and signal fields, Eqs. (1) must be solved simultaneously with the Maxwell equation. With the electric-field defined by $E_j = \mathcal{E}_j \exp[i(k_j - \omega_j t)] + \text{c.c.}$, we obtain

$$i \left(\frac{\partial}{\partial z} + \frac{1}{v_g^j} \frac{\partial}{\partial t} \right) \mathcal{E}_j + \frac{\omega_j}{2c} \chi_j \mathcal{E}_j = 0, \quad (j = p, s) \quad (2)$$

obtained under slowly-varying amplitude approximation, where v_g^j is the group velocity, generally defined as $v_g^j = c/(1+n_g^j)$ with $n_g^j = \text{Re}[\chi_j]/2 + (\omega_j/2)(\partial \text{Re}[\chi_j]/\partial \omega)|_{\omega=\omega_j}$ being the group index. Susceptibilities of the two weak fields are defined by $\chi_{p,s} = N_a D_0 a_2 a_{3,4}^*/(\epsilon_0 \mathcal{E}_{p,s})$ ($D_{23} \simeq D_{24} = D_0$), with N_a the atomic concentration.

We assume that atoms are initially populated in the ground state $|1\rangle$. For large one-photon detunings δ_1 and $\delta_1 + \Delta$ the ground-state depletion is not significant, i.e. $a_1 \simeq 1$. However, in order to take into account the nonlinear effect, we need to consider the higher-order contribution of a_1 , which can be obtained by using the condition $\sum_{i=1}^4 |a_i|^2 = 1$. Meanwhile, we assume that the

typical temporal duration of the probe and signal fields is long enough so that we can solve the equations adiabatically. With these considerations, we obtain the expressions of γ_1 and electric susceptibilities of the system

$$\gamma_1 = \gamma_2(G_1 + G_2) + \gamma \left[\frac{G_1}{\delta_2^2} + \frac{G_2}{(\delta_2 - \Delta)^2} \right] \times (|\Omega_p|^2 + |\Omega_s|^2), \quad (3)$$

and

$$\chi(\omega_j) \simeq \chi_j^{(1)} + \chi_j^{(3,s)} |\mathcal{E}_j|^2 + \chi_j^{(3,c)} |\mathcal{E}_{j'}|^2, \quad (4)$$

with $j, j' = p, s$ ($j \neq j'$) and

$$\chi_j^{(1)} \simeq -\kappa \left(\frac{G_1}{\delta_2 - i\gamma/2} + \frac{G_2}{\delta_2 - \Delta - i\gamma/2} \right), \quad (5a)$$

$$\chi_j^{(3,s)} = \chi_j^{(3,c)} \simeq \kappa' \left(\frac{G_1}{\delta_2 - i\gamma/2} + \frac{G_2}{\delta_2 - \Delta - i\gamma/2} \right) \times \left[\frac{G_1}{\delta_2^2} + \frac{G_2}{(\delta_2 - \Delta)^2} \right]. \quad (5b)$$

Here, $\chi_j^{(1)}$, $\chi_j^{(3,s)}$, and $\chi_j^{(3,c)}$ determine the linear, self-, and cross-Kerr nonlinear responses of the system. The constants in (3) and (5) are defined by $G_1 = |\Omega_{P1}|^2/\delta_1^2$, $G_2 = |\Omega_{P2}|^2/(\delta_1 + \Delta)^2$, $\kappa = \mathcal{N}_a |D_2|^2/(\hbar\epsilon_0)$, and $\kappa' = \mathcal{N}_a |D_2|^4/(\hbar^3\epsilon_0)$. We should also mention that in order to obtain simplified expressions of γ_1 [i.e. Eq. (3)] and third-order susceptibility [i.e. Eq. (5b)], we have taken $\delta_p = \delta_s = \delta_2$ and $\gamma_3 \simeq \gamma_4 = \gamma$, and used the conditions $\gamma_2^2 \ll \delta_1^2$, $\gamma^2 \ll \delta_2^2$, $\gamma^2 \ll (\delta_2 - \Delta)^2$, and $G_{1,2} \ll 1$. The real and imaginary parts of $\chi_j^{(1)}$ denote the phase shift per unit length and absorption or gain, respectively. From the expression of Eq. (5b), we see that the linear susceptibility for both the probe and signal fields have two Raman resonances, which contribute from two pump fields. If $\delta_2 = \Delta/2$ and the intensities of the two pump fields are well adjusted so that $G_1 = G_2 = G$, one has $\text{Re}[\chi_j^{(1)}] = 0$, and hence a gain-dependent linear phase can be completely removed [26]. In this case, $2\text{Im}[\chi_j^{(1)}] \simeq -8\kappa G\gamma/\Delta^2$ describes the intensity gain acquired by two weak fields. This is fundamentally different from all EIT-based systems which are inherently absorptive. The above choice of two-mode pump intensities and two-photon detuning also yields $\text{Re}[\chi_j^{(3)}] = 0$ and $2\text{Im}[\chi_j^{(3)}] \simeq 64\kappa' G^2\gamma/\Delta^4$, i.e. a zero nonlinear phase shift and a nonzero nonlinear intensity absorption. Therefore, in order to obtain a nonzero nonlinear phase shift, we need to slightly disturb the conditions $\delta_2 = \Delta/2$ or $G_1 = G_2 = G$.

In Fig. 2, we show the results of direct simulations of Eqs. (1) with a set of practical parameters given in the caption. The initial conditions are $a_1 = 1$ and $a_2 = a_3 = a_4 = 0$. The dependence of atomic probability amplitudes a_l ($l=1-4$) and quantity $\sum_{i=1}^4 |a_i|^2$ on time are illustrated. We can see that the condition $\sum_{i=1}^4 |a_i|^2 = 1$ is satisfied in a rather long time.

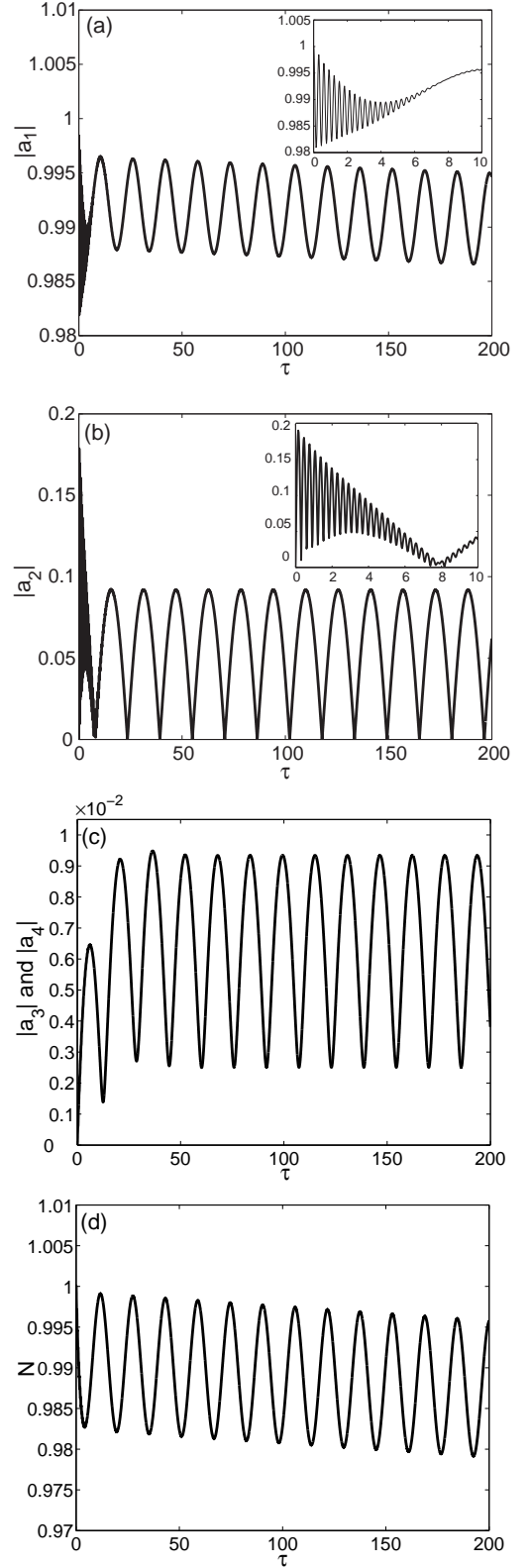


FIG. 2: The results of direct simulations of Eqs. (1) with the initial conditions $a_1 = 1$ and $a_2 = a_3 = a_4 = 0$. (a) The curves of $|a_1|$ versus τ . The inset shows the details for $\tau \in [0, 10]$. (b) The curves of $|a_2|$ versus τ . The inset shows the details for $\tau \in [0, 10]$. (c) The curves of $|a_j|$ ($j = 3, 4$) versus τ . (d) The curves of N versus τ . Here, $N \equiv \sum_{i=1}^4 |a_i|^2$ and $\tau \equiv \Omega_{P1}t$. The parameters are given by $\gamma_2 = 36$ MHz, $\gamma = 10$ MHz, $\delta_1 = 1.0 \times 10^9$ s $^{-1}$, $\delta_2 = 1.0 \times 10^7$ s $^{-1}$, $\Delta = 2.0 \times 10^7$ s $^{-1}$, $\Omega_{P1} = 5.0 \times 10^7$ s $^{-1}$, $\Omega_{P2} = 5.1 \times 10^7$ s $^{-1}$, and $\Omega_p = \Omega_s = 1.0 \times 10^6$ s $^{-1}$. $\gamma_1 = 0.2$ MHz is obtained by Eq. (3).

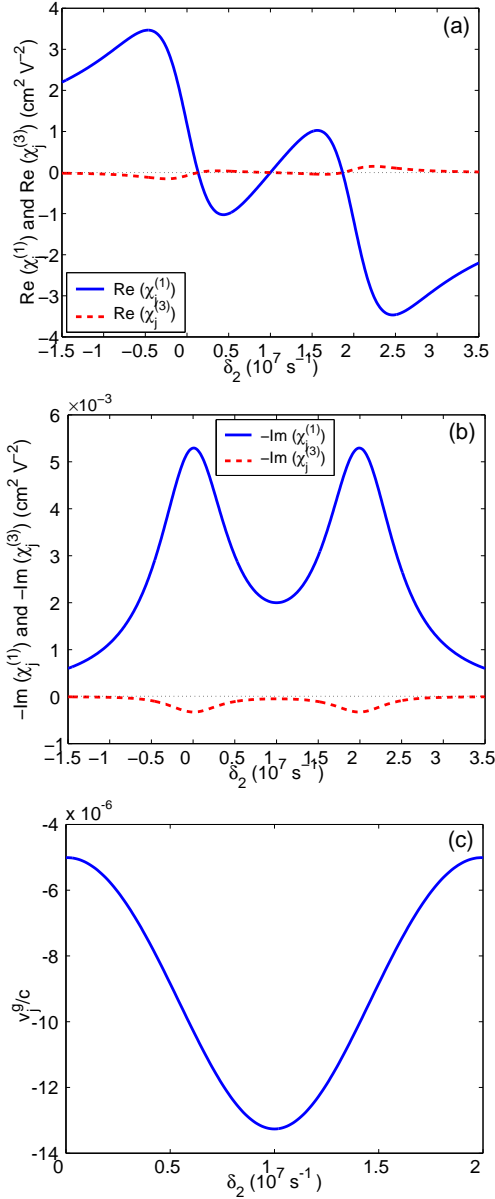


FIG. 3: (color online) (a) The curves of $\text{Re}(\chi_j^{(1)})$ (solid line) and $\text{Re}(\chi_j^{(3)})$ (dashed line) versus δ_2 . (b) The curves of $-\text{Im}(\chi_j^{(1)})$ (solid line) and $-\text{Im}(\chi_j^{(3)})$ (dashed line) versus δ_2 . (c) The curve of v_g^j/c versus δ_2 . The parameters are given by $\gamma_2 = 36$ MHz, $\gamma = 10$ MHz, $\delta_1 = 1.0 \times 10^9$ s $^{-1}$, $\Delta = 2.0 \times 10^7$ s $^{-1}$, $\Omega_{P1} = 5.0 \times 10^7$ s $^{-1}$, $\Omega_{P2} = 5.1 \times 10^7$ s $^{-1}$, $\mathcal{N}_a = 1.44 \times 10^{13}$ cm $^{-3}$, and $D_0 = 2.54 \times 10^{-27}$ C cm.

In Fig. 3(a) [Fig. 3(b)], we show the curves of $\text{Re}(\chi_j^{(1)})$ [$-\text{Im}(\chi_j^{(1)})$] and $\text{Re}(\chi_j^{(3)})$ [$-\text{Im}(\chi_j^{(3)})$] versus δ_2 with a set of practical parameters given in the caption [31]. A gain doublet structure in the spectrum can be apparently observed [see panel (b)], where a gain minimum can be acquired at $\delta_2 = \Delta/2$. Thus, when working near the gain minimum within the hole, a rapid increase of light intensity appeared in the ARG system can be effectively

avoided. In Fig. 3(c), we show the curves of v_g^j/c versus δ_2 . The group velocity is negative (with a small absolute value) corresponding the superluminal propagation.

Now we present the expressions of group velocities for both weak fields, which are defined by $v_g^j = c/(1 + n_g^j)$ ($j = p, s$). As we know, the group velocities of two light pulses must be comparable in order to achieve an effective CPM [12]. In our system, the group indexes of the probe and signal fields are given by

$$n_g^j \simeq -\frac{\kappa\omega_j}{2} \left[\frac{G_1}{\delta_2^2} + \frac{G_2}{(\delta_2 - \Delta)^2} \right]. \quad (6)$$

Because in our system $\omega_p \approx \omega_s$, we have $v_g^p \approx v_g^s$, and hence the group velocity matching is automatically satisfied. In addition, since $n_g^j \ll -1$ (due to the large values of ω_j), both group velocities are negative, i.e., the probe and signal fields travel with superluminal propagating velocities.

III. TWO-QUBIT POLARIZATION PHASE GATES AND HIGHLY ENTANGLED PHOTONS

The prototype of optical implementation of a two-qubit gate is the QPG in which one qubit gets a phase shift conditional to the other qubit state according to the transformation $|i\rangle_1|j\rangle_2 \rightarrow \phi_{ij}|i\rangle_1|j\rangle_2$, where $i, j = 0, 1$ denote logical qubit bases. This gate becomes universal when $\phi_{11} + \phi_{00} - \phi_{10} - \phi_{01} \neq 0$ [32].

We choose two orthogonal polarization states $|\sigma^-\rangle$ and $|\sigma^+\rangle$ to encode binary information for each qubit. The scheme shown in Fig. 1 is completely implemented only if both probe and signal fields have the “right” polarization states. When both of two weak fields have “wrong” polarization states, there is no sufficiently close excited state to which levels |3⟩ and |4⟩ can couple, and hence the probe and signal fields will only acquire the trivial vacuum phase shift $\phi_0^j = k_j L$. Here $k_j \equiv \omega_j/c$ ($j = p, s$), and L denotes the length of the medium. When one of the two weak fields have “wrong” polarization state, say for a σ^- -polarized probe field, there is no sufficiently close excited state to which levels |3⟩ can couple and the signal field subjects to the Λ -configuration constituted by |1⟩, |2⟩, and |4⟩ levels. Thus the signal field experiences a self-Kerr effect and acquires a nontrivial phase shift ϕ_1^s , while the probe field acquires only a vacuum phase shift ϕ_0^p . When only the probe and the signal fields have “right” polarization states, they all acquire nontrivial phase shifts ϕ_2^p and ϕ_2^s , respectively.

Assume that the input probe and signal pulses can be treated as polarized single photon wave packets, expressed as a superposition of the circularly polarized states, i.e. $|\psi\rangle_j = 1/\sqrt{2}|\sigma^-\rangle_j + 1/\sqrt{2}|\sigma^+\rangle_j$ ($j = p, s$). Here $|\sigma^\pm\rangle_j = \int d\omega \xi_j(\omega) a_\pm^\dagger(\omega) |0\rangle$ with $\xi_j(\omega)$ being a Gaussian frequency distribution of incident wave packet centered at frequency ω_j . The photon field operators undergo a transformation while propagating through the atomic medium of length L , i.e. $a_\pm(\omega) \rightarrow$

$a_{\pm}(\omega) \exp\{i\omega/c \int_0^L dz n_{\pm}(\omega, z)\}$. Assuming $n_{\pm}(\omega, z)$ (the real part of the refractive index) varies slowly over the bandwidth of the wave packet centered at ω_j , one gets $|\sigma^{\pm}\rangle_j \rightarrow \exp(-i\phi_{\pm}^j)|\sigma^{\pm}\rangle_j$, with $\phi_{\pm}^j = \omega_j n_{\pm}(\omega_j, z)L/c$. Thus, the truth table for a polarization two-qubit QPG using the present configuration is given by

$$|\sigma^{-}\rangle_p|\sigma^{+}\rangle_s \rightarrow \exp[-i(\phi_0^p + \phi_0^s)]|\sigma^{-}\rangle_p|\sigma^{+}\rangle_s, \quad (7a)$$

$$|\sigma^{-}\rangle_p|\sigma^{-}\rangle_s \rightarrow \exp[-i(\phi_0^p + \phi_1^s)]|\sigma^{-}\rangle_p|\sigma^{-}\rangle_s, \quad (7b)$$

$$|\sigma^{+}\rangle_p|\sigma^{+}\rangle_s \rightarrow \exp[-i(\phi_1^p + \phi_0^s)]|\sigma^{+}\rangle_p|\sigma^{+}\rangle_s, \quad (7c)$$

$$|\sigma^{+}\rangle_p|\sigma^{-}\rangle_s \rightarrow \exp[-i(\phi_2^p + \phi_2^s)]|\sigma^{+}\rangle_p|\sigma^{-}\rangle_s, \quad (7d)$$

where $\phi_0^j = k_j L$, $\phi_1^j = k_j L(1 + 2\pi\chi_j^{(1)}) + \phi^{(j,s)}$, and $\phi_2^j = \phi_1^j + \phi^{(j,c)}$, with

$$\phi^{(j,s)} = k_j L \frac{\pi^{3/2} \hbar^2 |\Omega_j|^2}{4|D_2|^2} \text{Re}[\chi_j^{(3,s)}], \quad (8a)$$

$$\phi^{(j,c)} = k_j L \frac{\pi^{3/2} \hbar^2 |\Omega_{j'}|^2}{4|D_2|^2} \text{Re}[\chi_j^{(3,c)}] \frac{\text{erf}(\xi_{jj'})}{\xi_{jj'}}, \quad (8b)$$

contributed respectively by self-phase modulation (SPM) and cross-phase modulation (CPM), where $\xi_{jj'} = \sqrt{2}L(1 - v_g^j/v_g^{j'})/(\tau_j v_g^j)$, with τ_j being the width of the pulse. If group velocity matching is satisfied, i.e. $\xi_{jj'} \rightarrow 0$, $\text{erf}[\xi_{jj}]/\xi_{jj}$ reaches its maximum value $2/\sqrt{\pi}$.

From Eq. (7), we can compute the degree of entanglement of the two-qubit state by using the entanglement of formation. For an arbitrary two-qubit system, it is given by [33]

$$E_F(C) = h\left(\frac{1 + \sqrt{1 - C^2}}{2}\right), \quad (9)$$

where $h(x) = -x \log_2(x) - (1-x) \log_2(1-x)$ is Shannon's entropy function, C is the concurrence given by $C(\hat{\rho}) = \max\{0, \lambda_1 - \lambda_2 - \lambda_3 - \lambda_4\}$. Here λ_i 's are square roots of eigenvalues of the matrix

$$\hat{\rho} \tilde{\rho} = \hat{\rho} \hat{\sigma}_y^p \otimes \hat{\sigma}_y^s \hat{\rho}^* \hat{\sigma}_y^p \otimes \hat{\sigma}_y^s \quad (10)$$

in decreasing order. The density matrix $\hat{\rho}$ in Eq. (10) can be directly obtained by using Eq. (7), the quantity $\tilde{\rho}$ ($\hat{\rho}^*$) means the transpose (complex conjugation) of $\hat{\rho}$, and $\hat{\sigma}_y$ denotes the y -component of the Pauli matrix.

Eq. (7) supports a universal QPG if the conditional phase shift [32]

$$\begin{aligned} & (\phi_0^p + \phi_0^s) + (\phi_2^p + \phi_2^s) - (\phi_0^p + \phi_1^s) - (\phi_1^p + \phi_0^s) \\ & = \phi^{(p,c)} + \phi^{(s,c)} \end{aligned} \quad (11)$$

is non-zero. From this formula, we see that only the phase shifts due to the CPM effect contribute to the conditional phase shifts.

Now we provide a practical set of parameters corresponding to typical values of ^{87}Rb atoms in room temperature. The decay rate of the lower states, i.e. $|3\rangle$ ($5^2S_{1/2}$, $F = 2$, $m = -1$) and $|4\rangle$ ($5^2S_{1/2}$, $F = 2$, $m = 1$),

is $\gamma = 300$ Hz. The hyperfine splitting between the lower states can be adjusted by the intensity of an externally applied magnetic field. For a magnetic field ≈ 340 G we obtain the splitting ≈ 3.8 GHz. The decay rate of the higher state $|2\rangle$ ($5^2P_{1/2}$, $F = 2$, $m = 0$) is $\gamma_2 = 36$ MHz. The other parameters are taken the same with those used in Fig. 2, as well as $\delta_2 = 0.8 \times 10^7$ s $^{-1}$. With the given parameters, we obtain that $\chi_j^{(1)} = -0.10 \times 10^{-2} - i0.85 \times 10^{-7}$ and $\chi_j^{(3)} = 0.34 \times 10^{-4} + i0.28 \times 10^{-8}$ cm 2 V $^{-2}$. We note that the imaginary parts of the susceptibilities are much smaller than those of the real parts due to the conditions $\gamma_2 \ll \delta_1$, $\gamma \ll \delta_2$, and $\delta_2 \neq \Delta/2$. A very small total gain effect remains after the balance of the linear gain and nonlinear absorption. The real parts of the third-order susceptibilities is about $\sim 10^{13}$ times larger than those measured for usual nonlinear optical materials, i.e., a giant enhancement of CPM can be achieved in our system. The group velocities of the both probe and signal fields are very well matched, with the values

$$v_g^p \approx v_g^s = -0.94 \times 10^{-5} c, \quad (12)$$

corresponding to indeed a superluminal propagation.

In Fig. 4(a), we have shown the calculating result of degree of entanglement versus the propagation the device length L . We see that a nearly 100% degree of entanglement can be obtained at $L = 0.53$ cm. The reason for acquiring such a high degree of entanglement is due to the non-absorption feature of the system. Shown in Fig. 4(b) are the curves of CPM induced phase shifts $\phi^{(p,c)}$ and $\phi^{(s,c)}$ versus L . We see that a conditional phase shift $\phi^{(p,c)} + \phi^{(s,c)}$ up to π radians can be obtained at $L \simeq 0.53$ cm, corresponding to the point of the maximum entanglement in Fig. 4(a). In Fig. 4(c), we show the curves of $\phi^{(p,c)}$ and $\phi^{(s,c)}$ versus δ_2 at $L = 0.53$ cm.

The probe and signal fields can have a mean amplitude of about one photon when these beams are focused or propagate in a tightly confined waveguide (e.g. hollow-core photonic crystal fibers [34]). With the above parameters, we obtain the intensities of the probe (I_p) and signal (I_s) fields, given by $I_p \approx I_s = 0.23 \times 10^{-6}$ W cm $^{-2}$ when $\Omega_p \approx \Omega_s = 1.0 \times 10^6$ s $^{-1}$. We remark that the intensity of a single 800-nm photon per nanosecond on the area of $1 \mu\text{m}^2$ is $I_{ph} = 2.5 \times 10^{-2}$ W cm $^{-2}$. This shows that our scheme can indeed make a polarization QPG with π conditional phase shift possible with single photon wave packets. Based on the superluminal propagating velocities and the enhanced CPM, the probe and signal fields acquire nontrivial nonlinear phase shifts when both of them have "right" polarization states in a fast response time and a short propagation distance, which allow us to implement a rapidly responding phase gate. For instance, if the group velocity of the probe and signal waves are reduced $10^{-4}c$ when using the EIT-based scheme, these waves will take around 180 ns to pass the device (for $L = 0.53$ cm) during which the nonlinear phase-shifting probe and signal fields must be present all the time. However, to acquire the same amount of the nonlinear phase

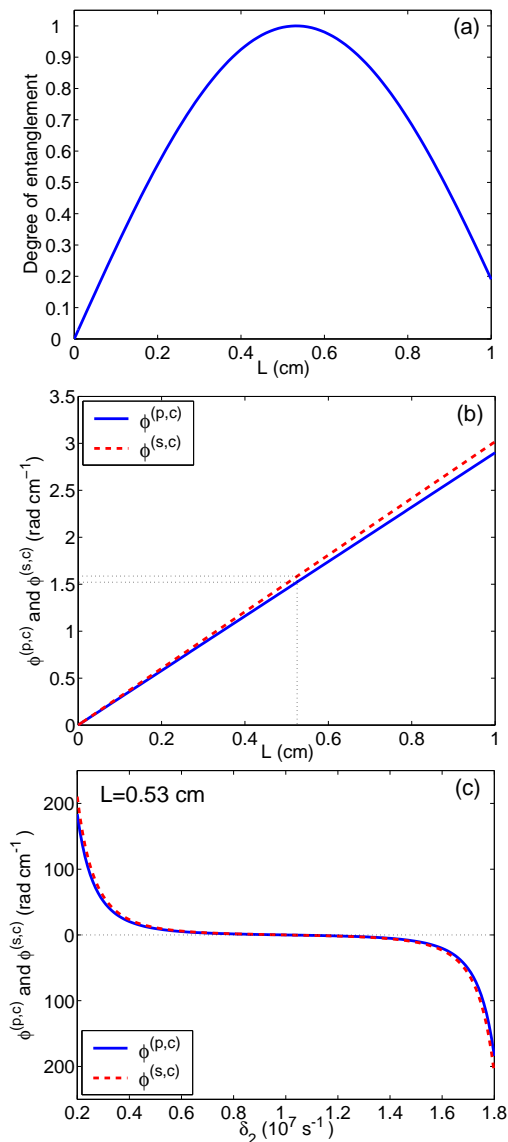


FIG. 4: (color online) (a) The degree of entanglement versus the device length L . (b) The curves of $\phi^{(p,c)}$ and $\phi^{(s,c)}$ versus L . A conditional phase shift $\phi^{(p,c)} + \phi^{(s,c)}$ up to π radians can be obtained at $L \simeq 0.53$ cm. (c) The curves of $\phi^{(p,c)}$ and $\phi^{(s,c)}$ versus δ_2 at $L = 0.53$ cm. The parameters are given in the text.

shift for the probe and signal waves in the present ARG system, the device transient time is only about 18 ps [35].

IV. DISCUSSION AND SUMMARY

Now we briefly discuss the Doppler effect due to the atom's thermal motion. Actually, our results can be readily generalized when an atom moves with a velocity V by the replacement $\delta_1 \rightarrow \omega_{21} - \omega_{P1} + k_{P1z}V_z$, $\delta_2 \rightarrow (\omega_{P1} - \omega_p) - \omega_{31} + (k_p - k_{P1})_z V_z = (\omega_{P1} - \omega_s) - \omega_{41} + (k_s - k_{P1})_z V_z$ (we assume all light fields propagate along the z -direction, as suggested in the inset of Fig. 1). The V_z -dependent terms obtained are then averaged over

a given thermal velocity distribution $f(V_z)$. From the above discussions, we see that the velocity-dependent effect in the two-photon detunings δ_2 in the copropagating case $k_{P1}k_j > 0$ is much smaller than those in the counter-propagating case $k_{P1}k_j < 0$. Consequently, the velocity-dependent effect or the Doppler effect in the two-photon detunings can be usually neglected compared with that in the one-photon detuning if we choose the waves to propagate in the same direction. Moreover, such effect in the one-photon detuning can also be efficiently suppressed if $\omega_{21} - \omega_{P1} \gg \omega_{P1z}V_z$, which is satisfied in our system.

The experimental demonstration of the phase gate requires the measurement of phase shifts, which will result in errors due to the fluctuations of light intensities and frequency detunings of the probe and signal fields. In order to minimize the effect of relative detuning fluctuations, one can take all lasers tightly phase locked to each other. The light intensity having fluctuations of 1% will yield an error less than 2% in the phase measurement.

We should point out that although CPM is a very promising candidate for the design of deterministic optical quantum phase gates, it still faces some challenges, which include: (i) How to achieve the sufficiently high single-photon intensity; (ii) How to overcome the phase noise induced by non-instantaneous nonlinear response inherent in resonant atomic systems; (iii) How to obtain a spatially homogeneous CPM necessary for effective entanglement between light pulses, etc. These problems are now actively investigated, and some methods for dealing with them have already been proposed [36]. On the other hand, in the present work we have treated the probe and signal fields in a classical way. Therefore, one would be easier to create the entanglement of macroscopic, coherent states rather than single photon states. A full quantum treatment is still necessary but beyond the scope of the present work.

To sum up, we have presented a scheme for obtaining entangled photons and quantum phase gates in a room-temperature four-state tripod-type atomic system with a two-mode ARG. We have analyzed the linear and nonlinear optical response of the ARG system and shown that the scheme is fundamentally different from those based on electromagnetically induced transparency and hence can avoid significant probe-field absorption as well as temperature-related Doppler effect. We have demonstrated that highly entangled photon pairs can be produced and rapidly responding polarization qubit quantum phase gates can be constructed based on the unique features of enhanced cross-phase modulation and superluminal probe-field propagation of the ARG system. The method provided here can also be extended to the study on multi-way entanglement and multi-qubit phase gates.

ACKNOWLEDGMENTS

Authors thank Y. Li and L. Deng for useful discussions and suggestions. This work was supported by NSF-

China under Grants No. 10434060 and No. 10874043, by the Key Development Program for Basic Research of China under Grants No. 2005CB724508 and No. 2006CB921104. C. H. was supported by the Fundação

para a Ciência e a Tecnologia (FCT) under Grant No. SFRH/BPD/36385/2007 and the Calouste Gulbenkian Foundation 2009.

-
- [1] M. A. Nielsen and I. L. Chuang, *Quantum Computation and Quantum Information* (Cambridge University Press, Cambridge, England, 2000).
- [2] M. Fleischhauer, A. Imamoglu and J. P. Marangos, *Rev. Mod. Phys.* **77**, 633 (2005), and references therein.
- [3] K. Hammerer, A. S. Sorensen, and E. S. Polzik, *Rev. Mod. Phys.* **82**, 1041 (2010), and references therein.
- [4] A. I. Lvovsky, B. C. Sanders, and W. Tittel, *Nat. Photon.* **3**, 706 (2009), and references therein.
- [5] R. Santra, E. Arimondo, T. Ido, C. H. Greene, and J. Ye, *Phys. Rev. Lett.* **94**, 173002 (2005).
- [6] T. Zanon-Willette, A. D. Ludlow, S. Blatt, M. M. Boyd, E. Arimondo, and J. Ye, *Phys. Rev. Lett.* **97**, 233001 (2006).
- [7] T. Hong, C. Cramer, W. Nagourney, and E. N. Fortson, *Phys. Rev. Lett.* **94**, 050801 (2005).
- [8] Y. Wu and L. Deng, *Phys. Rev. Lett.* **93**, 143904 (2004).
- [9] G. Huang, L. Deng, and M. G. Payne, *Phys. Rev. E* **72**, 016617 (2005).
- [10] H. Michinel and M. J. Paz-Alonso, and V. M. Pérez-García, *Phys. Rev. Lett.* **96**, 023903 (2006).
- [11] C. Hang, V. V. Konotop, and G. Huang, *Phys. Rev. A* **79**, 033826 (2009).
- [12] M. D. Lukin and A. Imamoglu, *Phys. Rev. Lett.* **84**, 1419 (2000).
- [13] A. Peng, M. Johnsson, W. P. Bowen, P. K. Lam, H.-K. Bachor, and J. J. Hope, *Phys. Rev. A* **71**, 033809 (2005).
- [14] I. Friedler, D. Petrosyan, M. Fleischhauer, and G. Kurizki, *Phys. Rev. A* **72**, 043803 (2005).
- [15] C. Ottaviani, D. Vitali, M. Artoni, F. Cataliotti and P. Tombesi, *Phys. Rev. Lett.* **90**, 197902 (2003).
- [16] S. Rebić, D. Vitali, C. Ottaviani, P. Tombesi, M. Artoni, F. Cataliotti and R. Corbalán, *Phys. Rev. A* **70**, 032317 (2004).
- [17] A. Joshi and M. Xiao, *Phys. Rev. A* **72**, 062319 (2005).
- [18] C. Hang, Y. Li, L. Ma, and G. Huang, *Phys. Rev. A* **74**, 012319 (2006).
- [19] If the group velocity of a light pulse is reduced by a factor of F from the speed of light in vacuum, the phase shift operation will be a factor of F slower [26].
- [20] R. Y. Chiao, *Phys. Rev. A* **48**, R34 (1993).
- [21] A. M. Steinberg and R. Y. Chiao, *Phys. Rev. A* **49**, 2071 (1994).
- [22] L. J. Wang, A. Kuzmich, and P. Pogariu, *Nature (London)* **406**, 277 (2000).
- [23] M. D. Stenner, D. J. Gauthier, and M. A. Neifeld, *Nature (London)* **425**, 695 (2003).
- [24] G. S. Agarwal and S. Dasgupta, *Phys. Rev. A* **70**, 023802 (2004).
- [25] K. J. Jiang, L. Deng, and M. G. Payne, *Phys. Rev. A* **76**, 033819 (2007).
- [26] L. Deng and M. G. Payne, *Phys. Rev. Lett.* **98**, 253902 (2007).
- [27] K. J. Jiang, L. Deng, E. W. Hagley, and M. G. Payne, *Phys. Rev. A* **77**, 045804 (2008).
- [28] G. Huang, C. Hang, and L. Deng, *Phys. Rev. A* **77**, 011803(R) (2008).
- [29] C. Hang and G. Huang, *Opt. Express* **18**, 2952 (2010).
- [30] R. W. Boyd and D. J. Gauthier, *Science* **326**, 1077 (2009).
- [31] Due to the symmetric configuration of the system, the linear and nonlinear susceptibilities of both the probe and signal fields are almost equal (see Eq. (5)). Hence, the curves plotted in Fig. 3 are valid for both the probe and signal fields.
- [32] Q. A. Turchette, C. J. Hood, W. Lange, H. Mabuchi, and H. J. Kimble, *Phys. Rev. Lett.* **75**, 4710 (1995).
- [33] V. Coffman, J. Kundu, and W. K. Wootters, *Phys. Rev. A* **61**, 052306 (2000).
- [34] M. Bajcsy, S. Hofferberth, V. Balic, T. Peyronel, M. Hafezi, A. S. Zibrov, V. Vuletic, and M. D. Lukin, *Phys. Rev. Lett.* **102**, 203902 (2009).
- [35] The lead time is typically about 10% of c . Thus the device transient time can be estimated quite accurately by using free-space speed of light [27].
- [36] K.-P. Marzlin, Z.-B. Wang, S. A. Moiseev, and B. C. Sanders, *J. Opt. Soc. B* **27**, A36 (2010).